Journal of Medicinal Chemistry

Article

Synthesis and Structure–Activity Relationship of a Novel Series of Aminoalkylindoles with Potential for Imaging the Neuronal Cannabinoid Receptor by Positron Emission Tomography

Peter G. Willis, Olga A. Pavlova, Svetlana I. Chefer, D. Bruce Vaupel, Alexey G. Mukhin, and Andrew G. Horti

J. Med. Chem., **2005**, 48 (18), 5813-5822• DOI: 10.1021/jm0502743 • Publication Date (Web): 06 August 2005

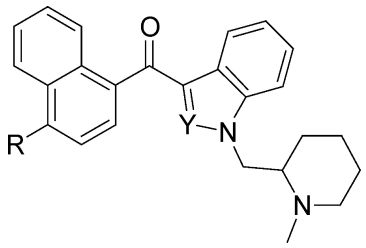

R=H, 4-OH, 4-CN, 4-F,
4-Br, 4-NO_2, 4-EtOH,
4-OMe, 2-Me, 6-OH, or 4-^{18}F
Y=CH or N

More About This Article

Additional resources and features associated with this article are available within the HTML version:

- Supporting Information
- Access to high resolution figures
- Links to articles and content related to this article
- Copyright permission to reproduce figures and/or text from this article

View the Full Text HTML

Synthesis and Structure−Activity Relationship of a Novel Series of Aminoalkylindoles with Potential for Imaging the Neuronal Cannabinoid Receptor by Positron Emission Tomography

Peter G. Willis,*,† Olga A. Pavlova,† Svetlana I. Chefer,† D. Bruce Vaupel,† Alexey G. Mukhin,† and Andrew G. Horti‡

Neuroimaging Research Branch, Intramural Research Program, National Institute on Drug Abuse, NIH, DHHS, 5500 Nathan Shock Drive, Baltimore, Maryland 21224, and Department of Radiology, Johns Hopkins University School of Medicine, 600 North Wolfe Street, Baltimore, Maryland 21287

Received March 25, 2005

A new series of CB_1 ligands with high binding affinity (K_i = 0.7−100 nM) and moderate lipophilicity ($cLogD_{7.4}$) in the range of 2.1−4.5 has been synthesized. A structure−activity relationship study demonstrated that for the studied set of aminoalkylindoles, the molecular dipole of the ground state conformation within the series was inversely related to the affinity. The racemic ligand with highest affinity (0.7 nM), 3-(4-fluoronaphthoyl)-1-(*N*-methylpiperidin-2-ylmethyl)indole, was radiolabeled with ^{18}F. This radioligand specifically labeled CB_1 receptors in mouse brain and accumulated in regions of high versus low CB_1 receptor density in a ratio of 1.6. The displaceable radioactivity of one enantiomer in the brains of mice determined in a pretreatment study using the CB_1 antagonist *N*-(piperidinyl)-5-(4-chlorophenyl)-1-(2,4-dichlorophenyl)-4-methyl-1*H*-pyrazole-3-carboxamide (SR141716) was nearly double that of the racemate for the same determination; therefore, the active enantiomer is a candidate for PET studies in animals. A pretreatement study for the other enantiomer found no displaceable radioactivity in the same group of mice; this result suggested the enantiomer was inactive.

Introduction

Cannabinoid receptors belong to the superfamily of G-protein coupled receptors. The cannabinoid subtype 1 receptor (CB_1) is found in the central nervous system as well as some nonneural tissues.[1] The other well-known cannabinoid receptor subtype (CB_2) is more localized in the immune system.[1,2] Δ^9-Tetrahydrocannabinol (Δ^9-THC; **1**), the principle physiologically active ingredient in marijuana, is known to activate CB_1 receptors, inducing the typical euphoric feelings associated with marijuana use. Figure 1 contains examples of the five major classes of natural and synthetic cannabinoid ligands including Δ^9-THC, the prototype of the classical cannabinoid ligand class. (1*R*,3*R*,4*R*)-3-[2-Hydroxy-4-(1,1,-dimethylheptyl)phenyl]-4-(3-hydroxypropyl)cyclohexan-1-ol (CP 55940; **2**) is an example of a nonclassical cannabinoid, as it only contains some of the structural motifs required for a classical cannabinoid. (*R*)-(+)-[2,3-dihydro-5-methyl-3-[(morpholinyl)methyl]-pyrrolo[1,2,3-*de*]-1,4-benzoxazinyl]-(1-naphthalenyl)methanone mesylate (WIN55212−2; **4**) and *N*-(piperidinyl)-5-(4-chlorophenyl)-1-(2,4-dichlorophenyl)-4-methyl-1*H*-pyrazole-3-carboxamide (SR141716; **5**) are examples of the aminoalkylindole (AAI) and 1,5-biarylpyrazole classes of cannabinoids, respectively. These two classes of ligands are purely synthetic in nature. Figure 1 also includes anandamide, **3**, a putative endogenous ligand for the cannabinoid receptor system.[3]

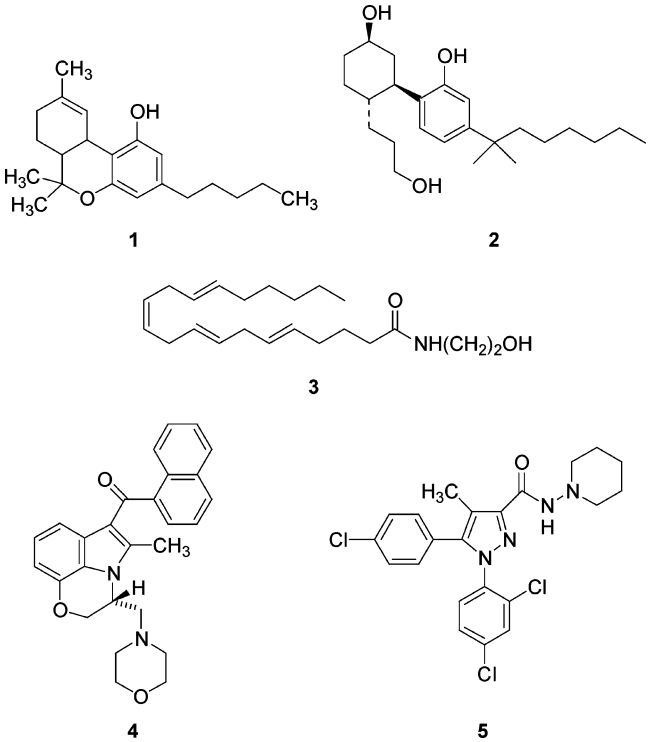

Figure 1. Five major classes of cannabinoid ligands. In left to right, top to bottom order: classical, nonclassical, endogenous, aminoalkylindoles, and 1,5-biarylpyrazoles.[4]

Cannabinoid receptor ligands produce several characteristic pharmacological effects.[1,5] Consequently, the implication of therapeutic applications for cannabinoids exists. Possibilities range from the treatment of nausea[6]

* Corresponding author. Tel.: +1-410-550-1440 ext. 331. Fax: +1-410-550-1441; E-mail: pwillis@intra.nida.nih.gov.
† National Institute on Drug Abuse.
‡ Johns Hopkins University School of Medicine.

10.1021/jm0502743 CCC: $30.25
Published on Web 08/06/2005

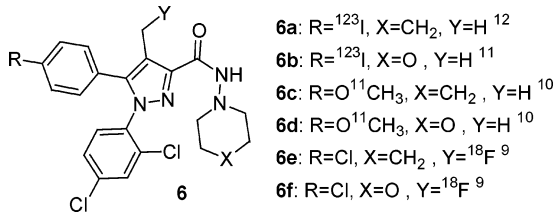

Figure 2. Representative CB_1 radiotracers.

and appetite control[7] to CNS disorders[8] and smoking cessation.[7] However, the role of cannabinoid receptors in the cause and treatment of these disorders is still not fully understood.[5]

The ability to image CB_1 receptors in the living human and animal brain using PET would provide the ability to conduct receptor studies in normal physiological conditions and in disease states. In addition, the development of a useful positron emission tomography (PET) radiotracer for CB_1 receptors may assist in the design and testing of promising pharmaceuticals targeting this receptor. Several analogues of **5** have been labeled with positron emitting isotopes and tested in animals,[9,10] (Figure 2) but the search for a ligand suitable for quantitative PET imaging and analysis of the CB_1 receptors[11,12] is a difficult one. Existing CB_1 radiotracers for in vivo imaging studies exhibit low ratios of radioactivity accumulation in regions of high versus low density of CB_1 receptors (1.6−2.5) due to their high lipophilicity and/or insufficient binding affinity.[9,10,12,13] It is apparent that currently available CB_1 ligands require optimization and improvement.

Efforts to develop PET and single photon emission computed tomography (SPECT) radioligands (Figure 2) have focused on finding new ligands with improved binding affinity and reduced lipophilicity.[9−11,14,15] Unfortunately, a recent structure−activity relationship (SAR) study with analogues of **5** demonstrated that for this subset of the 1,5-biarylpyrazole group, ligands with higher affinity tended to be more lipophilic or vice versa.[14]

Since ligands **6a**−**f** are of limited use due to their low affinity or high lipophilicity, other less lipophilic ligands may be more useful, for example the AAI class of ligands. Previous SAR studies with AAI have demonstrated the importance of the aminoalkyl tail, the alkyl chain connected to the nitrogen atom of the indole, for the binding affinity.[16] The highest affinity ligand within the series was 3-naphthoyl-1-(*N*-methylpiperidin-2-ylmethyl)indole, **8** (K_i = 0.9 nM), with the *N*-methylpiperidin-2-ylmethyl tail (Figure 3).[16] Modification of the tail is also an important tool in controlling lipophilicity of an AAI ligand.

In the present study we used compound **8** as a lead for development of high affinity CB_1 ligands with lower lipophilicity. The structure of compound **8** is comparable to the structure **7** (R = H) with the only dissimilarity being a different piperidine attached to the indole. A comparison of the two structural motifs reveals that both amines in the piperidine ring are tertiary and separated from the indole nitrogen by two carbons (shown in bold in Figure 3). In a SAR study by Eissenstat et al. improvements in the K_i of **7** were shown when small R groups were substituted for hydrogen.[17] The order of affinity for substitutions on **7** was R = OMe > Me > OH > H, which is also the same order as the length of the substituent R from long to short.

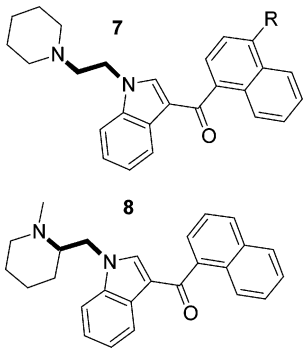

Figure 3. Structure of CB_1 ligands with SAR information.

Table 1. Synthesized CB_1 Ligands, Binding Affinity (K_i, determined in vitro), and Lipophilicity ($cLogD_{7.4}$)

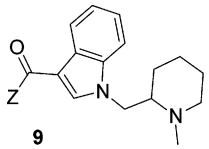

ligand	Z	K_i, nM	$cLogD_{7.4}$[a]
8[16]	1-naphthyl	0.9 ± 0.1	3.6
9a	4-Me-1-naphthyl	1.1 ± 0.1	4.0
9b	4-F-1-naphthyl	0.7 ± 0.1	3.8[b]
9c	4-Br-1-naphthyl	1.7 ± 0.2	4.5
9d	4-OMe-1-naphthyl	2.3 ± 0.3	3.6
9e	4-OH-1-naphthyl	2.2 ± 0.3	3.3
9f	4-CN-1-naphthyl	1.1 ± 0.1	3.3
9g	4-(2-hydroxyethyl)-1-naphthyl	1.3 ± 0.1	2.7
9h	6-OH-1-naphthyl	4 ± 1	2.8
9i	2-Me-1-naphthyl	7.8 ± 0.6	4.0
9j[18,19]	2-iodophenyl	1.2 ± 0.3	3.0
9k	*N*-naphthylamine	100 ± 7	3.0
9l	*N*-decahydroquinoline	12 ± 1	2.1
9m[c]	1-naphthyl	1.4 ± 0.1	3.1
9n[18,19]	4-NO_2-1-naphthyl	12.4[18,19]	3.5

[a] The dissociative partition coefficient $clogD_{7.4}$ was calculated using ACD/LogD Suite software. [b] The experimental $logD_{7.4}$ value as determined for [^{18}F]**9b** using a counting technique[19] in four assays is 2.54 ± 0.27. [c] Indazole instead of indole.

The goal of this research was to develop cannabinoid ligands with lower lipophilicity (logD) and increased affinity. The similarity of the structure of **7** R = H to **8** suggested that similar substitutions may also improve K_i. Therefore, a new series of derivatives **8**, **9a**−**n** (Table 1) was synthesized to test the effects of different substituents on affinity and lipophilicity. The ligand with the best combination of these characteristics was then labeled with a positron emitting isotope to test its potential as a PET radioligands for CB_1 receptors.

Results and Discussion

Structure−Activity Relationships (SAR). Twelve new AAI compounds with binding affinity and lipophilicity in the range of K_i = 0.7 to 100 nM and $logD_{7.4}$ = 2.1 to 4.5 were synthesized (Table 1). For all the structures in Table 1 where Z = 4-R-naphthyl (**9a**−**g**, **9n**), only R = F gave an improved K_i as compared with the lead compound **8**. The length of the R-group was defined by measuring the distance from the naphthalene ring to the far atom of the group when the system has been minimized with an AM1 semiempirical calculation

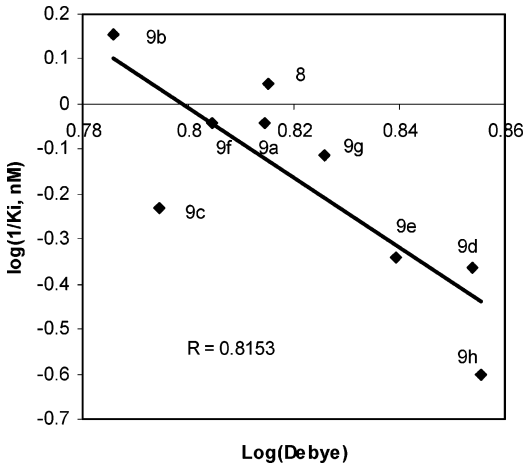

Figure 4. Correlation of the molecular dipole in log(Debye) with binding affinity, log(1/K_i, nM) for **8**, **9a**−**g**.

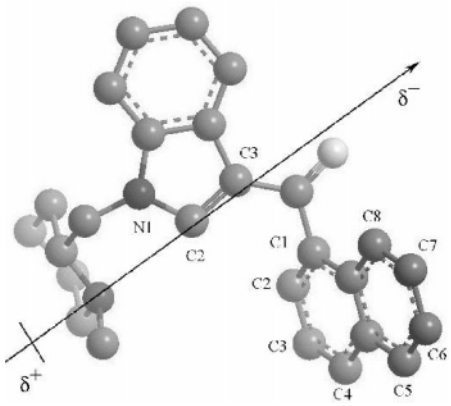

Figure 5. The global energy minimum conformation of compound **8**, and the direction of the molecular dipole as determined by an AM1 calculation.

and was assumed to be independent of the amino alkyl tail. Although the affinity appears to decrease for the larger substituents, the correlation of R length and K_i for **8**, **9a**−**o** was weak.

Comparisons of the molecular dipole versus binding affinity with CB_1 receptors showed a correlation within the tested set of structures (Figure 4). The R correlation factor was 0.82 for the relationship of log(Debye), a measure of the overall dipole strength, versus log(1/K_i), a measure of a ligand's affinity to CB_1 receptors. A dipole was calculated for the global energy minimum as determined by an AM1 calculation. The magnitude of the dipoles in this study indicated the difference in electron distribution of one side of the molecule versus the other side of the molecule (Figure 5). The calculation demonstrated that dipoles for **9b** and **8** were lower than those for **9d** and **9h**. The differences in the dipole of studied structures are primarily due to the changes in the properties of the substituent and the electron distribution in the naphthalene ring resulting from those changes.

Two points that do not seem to be adequately described by this correlation are the indazole **9m** and the 2-methylnaphthoyl derivative **9i**. The outlier **9m** suggests there are other negative interactions at the indazole nitrogen or that the effect is from a more localized dipole. **9i** has a more rigid structure than the other ligands, and has a torsion angle for naphthyl C2,C1,indole C3,C2 (Figure 5) that is 10° wider than those of **9b** or **8**. The observation of decreased affinity is consistent with the idea of a directing effect of the group ortho to the carbonyl group (e.g., the iodo group in **9j**, and the other benzyl group of the naphthalene in **8**).

This SAR is a refinement of the SAR from Shim et al. or Tetko et al., who examined many cannabinoid ligands including **7** and **8**, as mentioned in the Introduction.[17,21] These authors indicated that more negative electrostatic potential on carbon 4 of the naphthalene ring of **8** would increase affinity. The authors also suggest that a sterically forbidden region surrounds C2 and C3 of the naphthyl region. For ligand set **9**, only **9b** with a fluorine atom was an improvement over **8**. This can be explained by understanding that the substituent is a source of negative electrostatic potential that can change the size of the dipole with the strength of the potential and its location. Figure 5 shows the direction of the molecular dipole of **8** with the *z* component of the dipole vector of the dipole being zero due to the positioning of the molecule. The *z* axis is perpendicular to the plane of the paper; therefore, the vector shown in Figure 5 is parallel to the plane of the paper. Adding fluorine on carbon 4, as found on **9b**, will decrease the y component of this dipole versus that shown in Figure 5.

Possible explanations for why the correlation between dipole and affinity exist could come from the structure of the binding site for this molecule. For example, if a source of negative electrostatic potential on the receptor binding site exists near carbon 4, 5, or 6 of the naphthalene ring in a hypothetical binding site, large electronegative substituents would interfere with binding at this potential site. Or conversely, if a source of electropositive potential existed on the binding site near carbon 2 or 3, electronegative substituents (e.g. fluorine) nearer to the source of potential would increase potential. This hypothesis is consistent with the CoMFA model proposed by Shim et al. as explained above. The sterically forbidden region around C2 is seen in these data; however, it is most likely due to the large conformational changes caused by substitutions at C2 on the naphthalene ring. On the other hand, the explanation may come from an intrinsic affinity of the receptor for apolar ligands (e.g. anandamide or Δ^9-tetrahydrocannabinol). This explanation was made less likely due to the low correlation between lipophilicity and affinity.

Other possible relationships include one between lipophilicity and affinity cited by Katoch-Rouse et al. for 1,5-biarylpyrazole ligands.[14] This relationship indicated that increased affinity for this set of ligands led to increased lipophilicity. When the current set of ligands was checked for evidence of this relationship, none was found. From this it can be inferred that for the AAI class of ligands lipophilicity is not intrinsic to affinity.

It is noteworthy that the global minimum energy conformer of compounds **9g** and **2** can be easily superimposed as shown by the six pairs of atoms indicated in Figure 6. Kandemirli et al. uses a similar alignment to compare a mixed series of cannabinoids including **8** and **2**.[22] The similarity of the two ligands is an indicator that they may share some of the same van der Waals

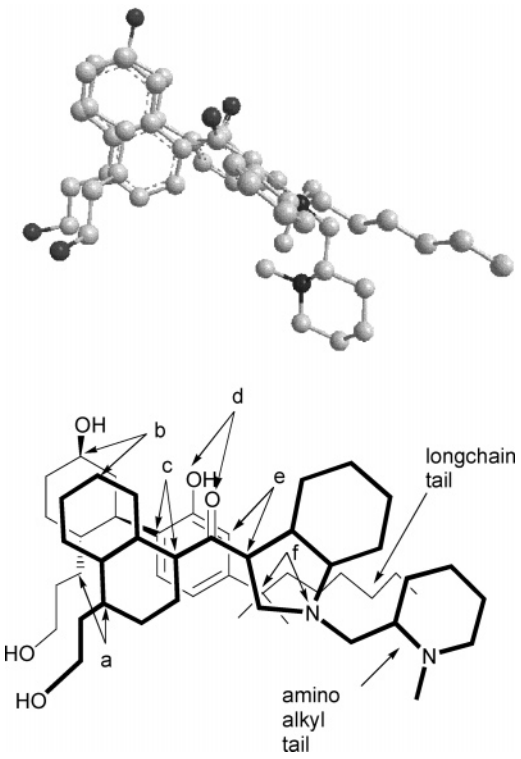

Figure 6. "Flat" and 3-D schemes of the superimposition of **8** and **2** by the six pairs of atoms (a−f).

Scheme 1. Synthesis of **8, 9a−j, n** by Friedel−Crafts Acetylation by Route 1[a]

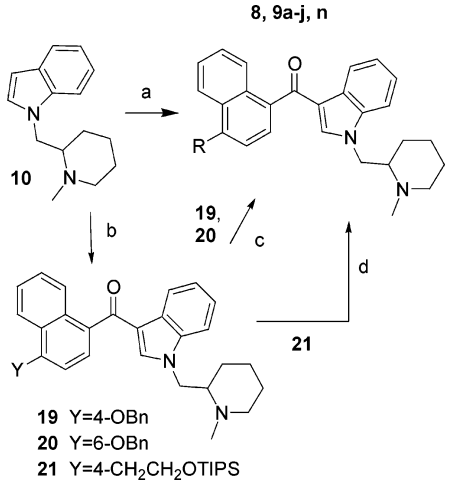

[a] Reagents: (a) (for **8, 9a−d**, **f**, **i**, and **n**) CH_2Cl_2, substituted naphthoyl chloride, $AlCl_3$; (b) (for **9e, h**, and **h**) [Bmin][PF_6], substituted naphthoyl chloride, heat; (c) (for **9e, h**) 10% Pd/C, ammonium formate; (d) (for **9g**) TBAF.

interactions. Figure 6 shows why it is reasonable to believe the two structures have conformational similarities, and why substitution at C4 of the naphthyl ring may give positive van der Waals interactions. Indole ligands with an aminoalkyl tail (e.g., ethyl-*N*-piperidine from **7**, or (*N*-methylpiperid-2-yl)methyl from **8**) or long chain tail (e.g., *n*-pentane) both give high affinity ligands, indicating the tails may have similar functions despite different tails.

Chemistry. The synthesis of the above ligands was accomplished through one of three routes. Route 1 (Scheme 1) consists of a Friedel−Crafts acetylation of an acid chloride synthon and indole **10**[16] (1-(*N*-methyl-

Scheme 2. Preparation of Indazole **9m** by Route 2[a]

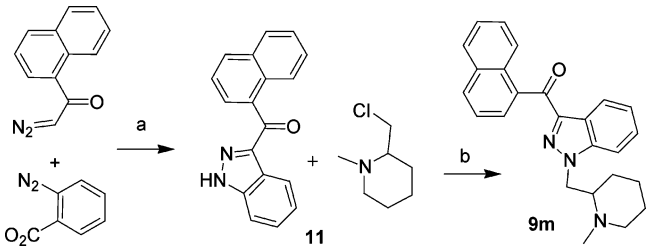

[a] Reagents: (a) refluxing CH_2Cl_2, 2.5 h; (b) DMF, NaH, RT, 2.5 d.

Scheme 3. Synthesis of Amide Derivatives **9k**, **l** by Route 3 with Acid Chloride **6**[a]

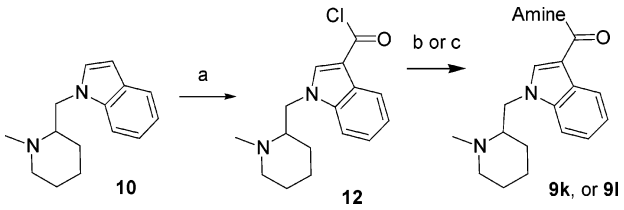

[a] Reagents: (a) trichloroacetyl chloride, NEt_3; NaOH; $SOCl_2$; (b)(for **9k**) 2-aminonaphthalene; or (c)(for **9l**) decahydroquinoline, CH_2Cl_2, NEt_3.

piperidin-2-ylmethyl)indole) under two different conditions. This route was used to synthesize **8**, **9a−j**, **n. 8**, **9a−d**, **f**, **i**, and **n** were prepared in the presence of Lewis acid. Compounds **9e**, **h**, and **g** were prepared in a solution of ionic liquid using the basic Friedel−Crafts reaction mechanism.[23] The ionic liquid[23] improved the yield over dipolar aprotic solvents and allowed the use of acid labile protecting groups, including benzyl and triisopropylsilyl (TIPS) ethers. Compounds **9e** and **9h** were synthesized under condition (b) with the corresponding benzyl derivatives **19** and **20**, and **9g** via the TIPS ether, **21**, and deprotected in a normal manner (Scheme 1).

Route 2 (Scheme 2) was used for the synthesis of the indazole, **9m**. When 2-diazocarboxylic acid was heated, benzyne was generated and underwent a 1,3-dipolar cycloaddition with 1-naphthyldiazomethyl ketone to generate **11**. Intermediate **11** was N-alkylated at position 1 on indazole with 2-chloromethyl-*N*-methylpiperidine.[24] Route 3 (Scheme 3) generated **9k** and **9l** from the acid chloride, **12**, and 2-aminonaphthalene, or decahydroquinoline via amide-forming conditions. The acid chloride **12** was synthesized from **10** by a procedure[25] used for a similar amine that involved an acetylation at indole carbon 3 with trichorloacetyl chloride, hydrolysis of the trichloroacetyl group, and conversion to the acid chloride.

Scheme 4 shows the synthesis of the acids used to make **9e**, **h**, and **g**. The precursor, **15**, for **9g** was generated from 1,4-dibromonaphthalene. This synthesis used a monoselective lithiation of 1,4-dibromonaphthalene. When 1 equiv of *n*-butyllithium was added to the reaction at −78 °C, monoalkalation is the primary product. The alcohol was then protected as the TIPS ether, **14**, and carboxylated to give the acid **15**. The synthesis of precursor **17**, shown in Scheme 4, for the synthesis of **9e** starts with the para bromination of 1-naphthol. By using acetonitrile as the solvent, bromination is directed to carbon 4, giving **16** in high yield.[26] The bromine could then be carboxylated to give

Scheme 4. Synthesis of a Precursor for Aminoalkylindole **9g, e, h**[a]

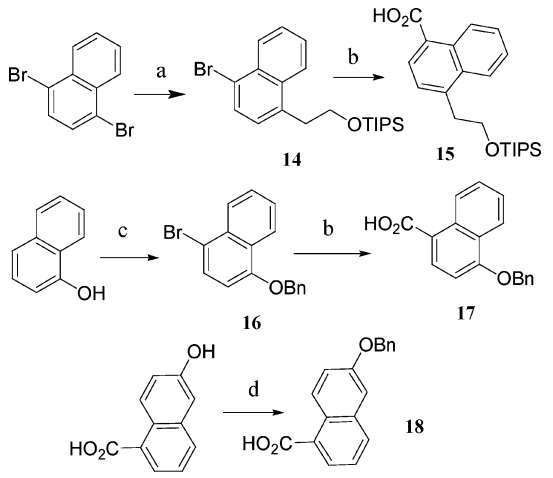

[a] Reagents: (a) *n*-BuLi, THF 1h, −78 °C; ethylene oxide, −78 °C to RT; NaH, TIPSCl; (b) *n*-BuLi, THF, 3 h, −78; CO_2(g), −78 °C to RT; (c) NBS, MeCN; BnBr, NaH, DMF; (d) KOH, DMF, BnBr; THF, K_2CO_3, reflux.

17. 6-Benzoxynaphthoic acid, **18**, a precursor for **9h**, was synthesized from 6-hydroxynaphthoic acid. **9n** was synthesized as described previously with minor modifications.[18]

In Vitro Binding Assay. The binding affinities of ligands **8**, **9a**−**n** for CB_1 receptors were determined by measuring the ability of each ligand to compete with [^{3}H]**2** binding in membrane fractions prepared from rat cerebellum (for data, see Table 1).

Lipophilicity. $LogD_{7.4}$ is a partition coefficient for charged species between octanol and water at pH 7.4. $logD_{pH}$ can be defined as: $logD_{pH} = log(\sum a_i^{org}/\sum a_i^{water})$ where a_i^{org} is the concentration of the ith microspecies in octanol and a_i^{water} is the concentration of the ith microspecies in water. The lipophilicity, $clogD_{7.4}$, was calculated with the ACD/LogD software for all the compounds in this study. Lipophilicity was also determined experimentally[20] for [^{18}F]**9b** (see Table 1).

Radiochemistry. Compound **9b** manifests the highest binding affinity with the series and moderate lipophilicity. Therefore, it was chosen as a candidate for radiolabeling with the PET isotope ^{18}F. The presence of a fluorine substituent in an activated position of the naphthalene ring suggested a straightforward radiosynthesis of [^{18}F]**9b** via nucleophilic radiofluorination.

Aromatic nitro groups readily undergo substitution reactions with the no-carrier-added (NCA) radiofluorination method when they are positioned para or ortho to an activating group.[27] **9n** contains an aromatic nitro substituent para to a carbonyl. With this in mind, the [^{18}F]**9b** was prepared with 10% radiochemical yield by the reaction of **9n** with Kryptofix222/K^{18}F complex and K_2CO_3 in DMSO followed by reverse phase semipreparative separation of the reaction mixture (Scheme 5). The specific activity of the final product was in the range of 2400−3200 mCi/μmol when prepared with 455−530 mCi [^{18}F]fluoride. Initially, the final product [^{18}F]**9b** was synthesized as racemic mixture. However, because previous evidence[16,18] demonstrated that only one of the AAI enantiomers exhibited high binding affinity at CB_1, we also performed chiral HPLC separation of the enantiomers, obtaining two nearly equal doses of radiolabeled compounds.

Scheme 5. Radiosynthesis of [^{18}F]**9b-1**, [^{18}F]**9b-2**[a]

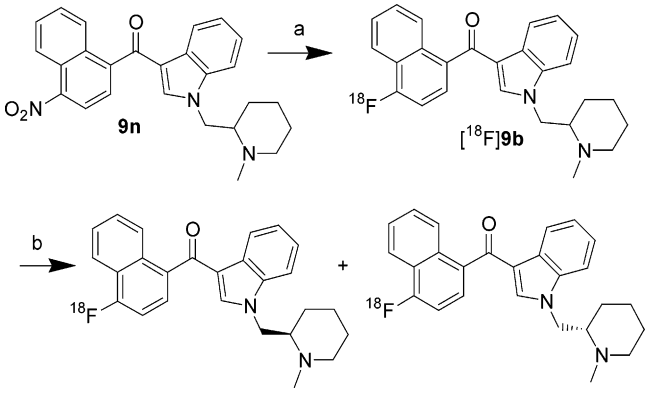

[a] (a) K222/K^{18}F, DMSO, 160 °C; (b) Chiralcel OD HPLC separation.

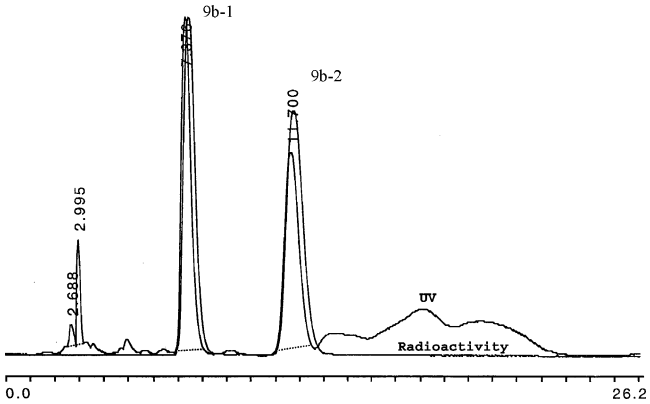

Figure 7. Chromatogram of chiral separation of racemic [^{18}F]**9b**, showing UV (254 nm) and radioactivity profiles. Peaks at 7.4 min (**9b-1**) and 11.7 min (**9b-2**) were approximately equal in area. Other peaks were nonradioactive byproducts.

In this study we did not decode the chiral structures of the enantiomers [^{18}F]**9b-1** and [^{18}F]**9b-2**. The two enantiomers came off the HPLC column (Figure 7) in the written order with [^{18}F]**9b-2** being the active isomer (see below). Pure samples of the nonlabeled enantiomers were prepared with a preparative chiral column and were analyzed for specific rotation. **9b-2** gave (+) rotation, the same sign as the *R* enantiomer for **8**, and **9j**.[16;18]

In Vivo Studies. Two separate studies were conducted in mice; the first one used the racemate [^{18}F]**9b**, and the second one tested enantiomers [^{18}F]**9b-1** and [^{18}F]**9b-2** separately. Racemic [^{18}F]**9b** showed moderate uptake into the whole mouse brain with maximum radioactivity accumulation of 0.033% (ID/kg)/g, at 7 min after administration (Figure 8). The maximum accumulation of radioactivity in the brain for racemic [^{18}F]**9b** is lower compared with some recent CB_1 tracers with antagonist properties, **6b**−**f**. The maximum radioactivity of compounds with similar maximum target to nontarget tissue ratios of radioactivity was 0.11 for **6b** or 0.18%(ID/kg)/g for **6f**.[12]

The patterns of regional distribution beginning 20 min after injection of [^{18}F]**9b** were consistent with the known distribution of CB_1 receptors.[28,29] Thus, the highest accumulation of radioactivity was consistently observed in the hippocampus and the lowest was seen

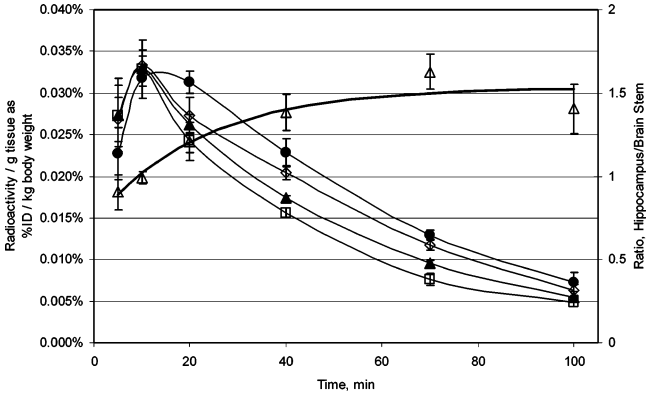

Figure 8. Kinetics of the regional distribution of the radioactivity of racemic [^{18}F]**9b** in the mouse brain: (●) hippocampus, (◊) striatum, (▲) total brain, (□) brain stem, (△) the ratio of hippocampus to brain stem radioactivity. Radioactivity accumulation is expressed as a percentage that is defined as the ratio of a concentration of radioactivity (Ci/g tissue) per injected dose radioactivity (Ci/kg body weight) times 100. Mice used in this test had an average body weight of 0.025 kg. Ratios shown represent target tissue (hippocampus) to nontarget tissue (brain stem). Each data point represents the mean ± SEM (n = 3).

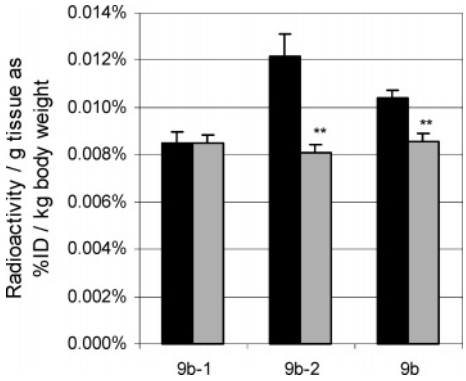

Figure 9. Inhibition of the radioactivity accumulation for the ^{18}F-labeled racemate **9b** and enantiomers **9b-1** and **9b-2** in mouse whole brain. Black bars indicate the control studies in which there was no pretreatment with **5**. Grey bars indicate the studies in which **5** was administered 15 min before the radiotracer to block the specific binding of radioligands to CB_1 receptors. Measurements were taken 60 min after injection of radiotracer for [^{18}F]**9b-1**, [^{18}F]**9b-2**, and [^{18}F]**9b**. Bars represent mean + SEM (n = 3). $^{**}P < 0.01$ as determined by Student's t-test indicate the significant differences of the radioactivity in studies with **5** pretreatment and the radioactivity of the control study.

in the brain stem. Following peak accumulation, a gradual decline in radioactivity was observed throughout the rest of the experiment. The hippocampus to brain stem ratio of accumulated radioactivity of racemic [^{18}F]**9b** reached a maximum value of 1.6 approximately 80 min after administration of the radioligand (Figure 8). This ratio is comparable to that of the less lipophilic radioligands for imaging CB_1, **6d** and **6f**.[11]

Preadministration of **5** (1 mg/kg), a selective CB_1 antagonist, significantly reduced the radioactivity of [^{18}F]**9b** in the mouse whole brain compared to the radioactivity in a control experiment without preadministration (Figure 9). This reduction, defined as the displaceable radioactivity, was significant and indicated that some fraction of the total radioactivity in the brain belongs to the specific binding of radioligand to CB_1

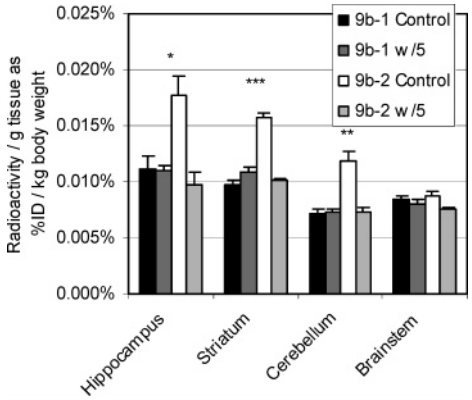

Figure 10. Inhibition of radioactivity accumulation of ^{18}F-labeled enantiomers, **9b-1** and **9b-2**, by **5** in brain regions with high CB_1 receptor density and in the brainstem in mice. For each enantiomer, **5** was administered 15 min before the radiotracer to block the specific binding of radioligands to CB_1. In control studies there was no pretreatment with **5**. Measurements were taken 60 min after injection of radiotracer. Bars represent mean + SEM (n = 3). $^{*}P < 0.02$, $^{**}P < 0.01$, and $^{***}P < 0.002$ as determined by Student's t-test indicate the significant differences between the radioactivity values of a control study with **9b-2** and the radioactivity values of the other studies in the corresponding tissues.

receptors. The enantiomers [^{18}F]**9b-1** and [^{18}F]**9b-2** were also tested. Preadministration of **5** did not have any effect on accumulation of [^{18}F]**9b-1**. In other words, there was no displaceable radioactivity. In contrast, a significant portion of the radioactivity of [^{18}F]**9b-2** was displaceable. For [^{18}F]**9b-2** the displaceable portion of the radioactivity nearly doubled compared to racemic [^{18}F]**9b**. Therefore, the results of pretreatment studies with **5** indicate that while [^{18}F]**9b-2** is an active radiotracer for CB_1 receptors, [^{18}F]**9b-1** is inactive.

The levels of radioactivity for the three regions with high CB_1 receptor density and the brainstem, shown in Figure 10, were compared in studies with and without **5** pretreatment. The values of target (hippocampus, striatum, and cerebellum) to nontarget (brainstem) ratio measured at 60 min after radioligand administration were (1.3, 1.2, 0.9) and (2.0, 1.8, 1.4) for **9b-1** and **9b-2**, respectively. The total radioactivity determined for the control study of [^{18}F]**9b-1** was comparable to the radioactivity determined for pretreatment studies with [^{18}F]**9b-1** and [^{18}F]**9b-2**. In contrast, the radioactivity determined for the control experiment of [^{18}F]**9b-2** was significantly greater than the other experiments, suggesting significant specific binding to CB_1 receptors. The results of these studies suggest that [^{18}F]**9b-2** has potential as a PET radioligand for studying CB_1, whereas [^{18}F]**9b-1** is a useful indicator of the nondisplaceable accumulation of radioactivity for [^{18}F]**9b-2**.

Conclusion

A novel series of 3-naphthoyl substituted AAIs with high affinity for CB_1 receptors and lipophilicity ($cLogD_{7.4}$) in the range of 2.7−4.5 was synthesized. A SAR of the studied set of AAIs, demonstrated that the affinity is inversely related to the size of the molecular dipole. This relationship was sustained even when substitution was not at naphthyl carbon four, i.e., compound **9h**.

Radioligand [^{18}F]**9b** specifically labels CB_1 receptors in mouse brain. Separation of and in vivo studies with

the two enantiomers of [^{18}F]**9b** demonstrated that only one of the enantiomers [^{18}F]**9b-2** exhibits specific binding to CB_1 receptors and therefore has potential as a PET radioligand. These results suggest that the inactive enantiomer [^{18}F]**9b-1** could provide a reasonable measurement of the nondisplaceable binding of the active enantiomer [^{18}F]**9b-2**.

Experimental Section

Chemistry. Unless specifically indicated, all reagents were purchased from Aldrich. All solvents used were ACS or HPLC grade. ^{1}H NMR spectra were recorded on a Bruker AM 300 (300 MHz) instrument; chemical shifts (δ) were recorded in parts per million (ppm) downfield from TMS. High-performance liquid chromatography (HPLC) analysis and purification were performed with a Rheodyne 7725 injector, a Waters 515 HPLC pump, and an in-line Waters 2487 dual λ absorbance detector (254 nm). HPLC chromatograms were recorded by a Waters Pump Control Module connected to a HP computer equipped with Waters Empower software program. Waters Symmetry C-18 (3.5 μm, 4.6 mm × 75 mm), Chiracel OD (10 μm, 4.6 mm × 250 mm), and Waters Nova-Pak C-18 radial compression (6 μm, 25 mm × 100 mm) columns were used in the HPLC analyses and preparative separations. Analytical thin-layer chromatography (TLC) was done on precoated plates of silica gel (0.25 mm, F254, Alltech). Flash chromatography was conducted using silica gel (230−400 mesh, Merck). Melting points were determined on a Mel-Temp II apparatus. Elemental analyses were performed by Quantitative Technologies, Inc. (QTI). The newly synthesized final compounds gave satisfactory elemental analyses results (C, H, N, F ±0.40%). The *c*log $D_{7.4}$ values were calculated using ACD/LogD Suite software (Advanced Chemistry Development Inc., Toronto, Canada).

Compounds **8** (AM251),[16] **9j**,[18] and **9n**[18] were synthesized using a procedure described elsewhere in the literature.

3-(4-Methynaphthoyl)-1-(*N*-methylpiperidin-2-ylmethyl)indole (9a). 4-Methylnaphthoic acid (206.6 mg, 1.110 mmol) was heated in 1.5 mL $SOCl_2$ at 70 °C for 2 h, evaporated under vacuum, and used as is for the next step. $AlCl_3$ (170.9 mg, 1.282 mmol) was stirred as a suspension in 2 mL CH_2Cl_2 for 15 min. The acid chloride was dissolved in 2 mL CH_2Cl_2, added to the suspension of aluminum chloride and stirred for 0.5 h. 1-(*N*-Methylpiperidin-2-ylmethyl)indole[16] (**10**) (129.6 mg, 0.567 mmol) in 1 mL CH_2Cl_2 was then added to the reaction dropwise at RT. The reaction was then warmed to 40 °C for 1 h, worked up with K_2CO_3, and extracted into CH_2Cl_2. The product was purified on silica with 3.75:1.75:0.5 hexane:$CHCl_3$:NEt_3. R_f was 0.26 in 6:4:1 hexane:$CHCl_3$:NEt_3. An oily solid was further purified by washing with hexane for an 82% yield (184.5 mg 0.465 mmol). mp = 123−4 °C, ^{1}H NMR (300 MHz, $CDCl_3$) δ 8.45 (m, 1H), 8.27 (d, J = 8 Hz, 1H), 8.19 (d, J = 8 Hz, 1H), 7.55 (m, 3H), 7.37 (m, 5H), 4.53 (dd, J = 4, 14 Hz, 1H), 3.87 (dd, J = 9, 14 Hz, 1H), 2.85 (d, J = 12 Hz, 1H), 2.78 (s, 3H) 2.41 (s, 3H), 2.37 (m, 1H), 2.12 (dt, J = 3, 12 Hz, 1H), 0.8−1.8 (m, 11H), Anal. ($C_{27}H_{28}N_2O$·0.09EtOAc) C, H, N.

3-(4-Fluoronaphthoyl)-1-(*N*-methylpiperidin-2-ylmethyl)indole (9b). 9b was prepared like that for **9a**, using 4-flouronaphthoic acid (97.0 mg, 0.510 mmol), 0.5 mL $SOCl_2$, $AlCl_3$ (78.3 mg, 0.587 mmol), and **10** (51.4 mg, 0.225 mmol). The product was purified on silica with 3.25:1.75:0.5 hexane:$CHCl_3$:NEt_3. R_f 0.19 in 6:4:1 hexane:$CHCl_3$:NEt_3. An oily solid was recovered and washed with hexane for a 76% yield. mp = 137 °C, ^{1}H NMR (300 MHz, $CDCl_3$) δ 8.56 (m, 1H), 8.27 (d, J = 8 Hz, 1H), 8.19 (d, J = 8 Hz, 1H), 7.63 (m, 3H), 7.37 (m, 4H), 7.19 (t, 1H), 4.53 (dd, J = 4, 14 Hz, 1H), 3.87 (dd, J = 9, 14 Hz, 1H), 2.85 (d, J = 12 Hz, 1H), 2.41 (s, 3H), 2.37 (m, 1H), 2.12 (dt, J = 3, 12 Hz, 1H), 0.8−1.8 (m, 11H), Anal. ($C_{26}H_{25}N_2OF$) C, H, N, F.

Product was separated into its two enantiomers on a ChiralPak OD HPLC column (semipreparative, 250 × 20 mm) 75:25:0.2 hexane:IPA:diethylamine eluent. Product was washed with hexane and dried under vacuum. Retention times were 14.8 min for the first component **9b-1** and 25.6 min for the second component **9b-2** with a flow rate of 10 mL/min. Fractions were collected, dried, and analyzed on an analytical ChiralPak OD column. Specific rotation for **9b-2** is $[\alpha]^{26}_D$ = +30.47 (*c* 0.105 in ethanol) and **9b-1** is $[\alpha]^{27}_D$ = −59.99 (*c* 0.130 in ethanol).

3-(4-Bromonaphthoyl)-1-(*N*-methylpiperidin-2-ylmethyl)indole (9c). 9c was prepared like that for **9a**, using 4-bromonaphthoic acid[30] (530.2 mg, 2.112 mmol), 6 mL $SOCl_2$, $AlCl_3$ (500 mg, 3.75 mmol), and **10** (242.2 mg, 1.060 mmol). The product was purified on silica with 3.75:1.75:0.5 hexane:$CHCl_3$:NEt_3. R_f 0.19 in 6:4:1 hexane:$CHCl_3$:NEt_3. **9c** was recovered as an oily solid which was purified by washing with hexane for a 67% yield. ^{1}H NMR (300 MHz, $CDCl_3$) δ 8.45 (m, 1H), 8.36 (d, J = 8 Hz, 1H), 8.20 (d, J = 8 Hz, 1H), 7.86 (d, 1H), 7.64 (td, 1H), 7.52 (m, 2H), 7.38 (m, 4H), 4.52 (dd, J = 4, 14 Hz, 1H), 3.85 (dd, J = 9, 14 Hz, 1H), 2.85 (d, J = 12 Hz, 1H), 2.38 (s, 3H), 2.35 (m, 1H), 2.11 (dt, J = 3, 12 Hz, 1H), 0.8−1.8 (m, 8H), Anal. ($C_{26}H_{25}BrN_2O$) C, H, N, Br.

3-(4-Methoxynaphthoyl)-1-(*N*-methylpiperidin-2-ylmethyl)indole (9d). 9d was prepared like that for **9a**, using 4-methoxynaphthoic acid (56.8 mg, 0.281 mmol), 0.5 mL $SOCl_2$, $AlCl_3$ (64.1 mg, 0.481 mmol), **10** (31.9 mg, 0.140 mmol). The reaction was purified on silica with 6:4:1 hexane:$CHCl_3$:NEt_3. R_f 0.11 in 6:4:1 hexane:$CHCl_3$:NEt_3. **9d** was recovered as an oily solid which was purified by washing with hexane for a 77% yield. mp = 143 °C, ^{1}H NMR (300 MHz, $CDCl_3$) δ 8.45 (m, 1H), 8.36 (d, J = 8 Hz, 1H), 8.20 (d, J = 8 Hz, 1H), 7.86 (d, 1H), 7.64 (td, 1H), 7.52 (m, 2H), 7.38 (m, 4H), 4.52 (dd, J = 4, 14 Hz, 1H), 3.85 (dd, J = 9, 14 Hz, 1H), 2.85 (d, J = 12 Hz, 1H), 2.38 (s, 3H), 2.35 (m, 1H), 2.11 (dt, J = 3, 12 Hz, 1H), 0.8−1.8 (m, 8H), Anal. ($C_{27}H_{28}N_2O_2$·0.2EtOAc) C, H, N.

3-(4-Cyanonaphthoyl)-1-(*N*-methylpiperidin-2-ylmethyl)indole (9f). 4-Cyanonaphthoic acid was made from 4-methylnaphthonitrile by a procedure from the cited literature[31] by a radical bromination of the aryl methyl, then conversion of the aryl bromide to an aldehyde by a nucleophilic reaction of hexamine with the aryl bromide and a hydrolytic workup. This aldehyde was converted to an acid with potassium permanganate. **9f** was prepared like that for **9a**, using the prepared 4-cyanonaphthoic acid (104.6 mg, 0.530 mmol), 2 mL $SOCl_2$, $AlCl_3$ (223.5 mg, 1.676 mmol), and **10** (73.9 mg, 0.320 mmol). Product was purified on silica with 6:4:1 then 5:5:1 hexane:$CHCl_3$:NEt_3 solvent system. R_f 0.16 in 6:4:1 hexane:$CHCl_3$:NEt_3. **9f** was recovered as an oily solid, which was purified by washing with hexane for a 35% yield. mp = 125 (dec) °C, ^{1}H NMR (300 MHz, $CDCl_3$) δ 8.42 (m, 1H), 8.36 (d, J = 8 Hz, 1H), 8.41 (d, J = 8 Hz, 1H), 8.12 (d, 1H), 8.00 (d, J = 7 Hz, 1H), 7.74 (td, J = 7, 1 Hz, 1H), 7.67 (d, J = 9 Hz, 1H), 7.59 (td, J = 1, 8 Hz, 1H), 7.40 (m, 3H), 7.33 (s, 1H), 4.51 (dd, J = 4, 14 Hz, 1H), 3.87 (dd, J = 9, 14 Hz, 1H), 2.83 (dt, J = 14, 7 Hz, 2H), 2.39 (s, 3H), 2.36 (m, 1H), 2.11 (dt, J = 3, 12 Hz, 1H), 0.8−1.8 (m, 11H), Anal. ($C_{27}H_{25}N_3O$·0.2EtOAc) C, H, N.

3-(2-Methylnaphthoyl)-1-(*N*-methylpiperidin-2-ylmethyl)indole (9i). 9i was prepared like that for **9a**, using 2-methylnaphthoic acid (216.0 mg, 1.160 mmol), 2 mL $SOCl_2$, $AlCl_3$ (223.5 mg, 1.676 mmol), and **5** (73.9 mg, 0.320 mmol). The final step was warmed to 70 °C for 3 h. **9i** was recovered as an oily solid, which was purified by crystallization with hexane for a 65% yield. mp = 160 °C, ^{1}H NMR (300 MHz, $CDCl_3$) δ 8.69 (b, 1H), 7.84 (d, 2H), 7.72 (t, 1H), 7.53−7.31 (m, 6H), 7.05 (b, 1H), 4.47 (bd, J = 14 Hz, 1H), 3.77 (b, 1H), 2.80 (b, 1H), 2.41 (s, 3H), 2.35 (bs, 4H), 2.08, Anal. ($C_{27}H_{28}N_2O$· 0.2EtOAc) C, H, N.

3-(4-Benzyloxynaphthoyl)-1-(*N*-methylpiperidin-2-ylmethyl)indole (19). 4-Benzyloxy-1-bromonaphthalene (**16**)[32] (200.1 mg, 0.6389 mmol) in 5 mL tetrahydrofuran was added to a solution of *n*-butyllithium (440 μL, 1.6 M) in 5 mL at −15 °C for 10 min, then stirred for another 30 min. Dried CO_2 was bubbled through the reaction for another 30 min. The product was acidified with $NaHSO_4$ and extracted into ether. 4-Benzyloxynaphthoic acid (**17**) was recovered pure by crystallization with hexane and ether in 45% yield. **17** (247.6 mg, 0.8897 mmol) was dissolved in 0.2 mL of thionyl chloride and 7 μL

DMF at room temperature for 2 h, then dried under vacuum. The resulting acid chloride and 425 mg of the ionic liquid 1-butyl-3-methylimidazolium hexafluorophosphate ([bmin]-[PF_6]) were heated to 150 °C in a sealed vial, and the product was purified by washing the ionic liquid with $CHCl_3$ and 1 N Na_2CO_3. **19** (360.4 mg, 0.7375 mmol) was obtained pure by flash chromatography with the solvent gradient 8:2:1 to 6:4:1 hexane:$CHCl_3$:NEt_3. R_f 0.15. ^{1}H NMR (300 MHz, $CDCl_3$) δ 8.48 (m, 1H), 8.32 (m, 1H), 8.29 (m, 1H), 7.53−7.31(m, 7H), 6.69 (d, J = 8 Hz, 1H), 4.60 (dd, J = 4, 14 Hz, 1H), 3.94 (dd, J = 9, 14 Hz, 1H), 2.94 (d, J = 12 Hz, 1H), 2.49 (m, 1H), 2.44 (s, 3H), 2.20 (dt, J = 5, 10 Hz, 1H), 0.98−1.71 (m, 11H)

3-(4-Hydroxynaphthoyl)-1-(*N*-methylpiperidin-2-ylmethyl)indole (9e). **19** (205.0 mg, 0.4195 mmol) was stirred under argon with 417.6 mg 10% Pd/C and 279.4 mg ammonium formate. After being stirred for 1 h, the mixture was filtered, diluted with EtOAc, and washed with (aq) K_2CO_3 and 3× DI water. **9e** was obtained as pale yellow oil in 78% yield. ^{1}H NMR (300 MHz, $CDCl_3$) δ 8.47 (m, 1H), 8.32 (m, 2H), 7.52 (d, J = 8 Hz, 1H), 7.28−7.49 (m, 6H), 6.72 (d, J = 8 Hz, 1H), 4.57 (dd, J = 4, 14 Hz, 1H), 3.92 (dd, J = 9, 14 Hz, 1H), 2.91 (d, J = 12 Hz, 1H), 2.44 (s, 4H), 2.17 (m, 1H), 0.75−1.72 (m, 9H). Anal. ($C_{26}H_{26}N_2O_2$·H_2O), C, H, N.

3-(Naphthoyl)-1-(*N*-methylpiperidin-2-ylmethyl)indazole (9m). 3-Naphthoyl indazole was made by a 1,3 dipolar cycloaddition of naphthoyldiazomethane and the benzyne equivalent, 2-diazobenzene carboxylic acid; physical data matched the literature.[33] Wet 2-diazocarboxylic acid was used in the first step of the reaction as the reagent becomes explosive upon drying. The indazole (47.9 mg, 0.176 mmol), *N*-methyl-2-chloromethylpiperidine (42.9 mg, 0.291 mmol), and NaH (11 mg) were stirred in anhydrous DMF at room temperature for 2 days, evaporated under vacuum, worked up with saturated $NaHCO_3$, and extracted into ether. The residue was purified by flash chromatography using 8:2:1 hexane:$CHCl_3$:NEt_3, yielding **9m** (17.3 mg, 0.0451 mmol) with an R_f of 0.30 in 6:4:1 hexane:$CHCl_3$:NEt_3. mp = 98−100 ^{1}H NMR (300 MHz, $CDCl_3$) δ 8.44 (d, 8 Hz, 1H), 8.34 (m, 1H), 8.03 (d, 8 Hz, 1H), 7.86−7.99 (m, 2H), 7.45−7.61 (m, 5H), 7.38 (m, 1H), 4.79 (dd, 5, 14 Hz, 1H), 4.32 (dd, 9, 14 Hz, 1H), 2.88 (d, 11 Hz, 1H), 2.66 (m, 1H), 2.41 (s, 3H), 2.19 (m, 1H), 0.8−1.8 (m, 11H). Anal. ($C_{25}H_{25}N_3O$·0.5EtOAc) C, H, N.

3-(Carboxy-1-aminonaphthyl)-1-(*N*-methylpiperidin-2-ylmethyl)indole (9k). 3-(Carboxylic acid)-1-(*N*-methylpiperidin-2-ylmethyl)indole (92.0 mg, 0.332 mmol) was stirred at room-temperature overnight with 74 μL thionyl chloride and 1 mL anhydrous $CHCl_3$, evaporated, and stirred with 1 mL methylene chloride, 60 μL NEt_3, and 1-aminonaphthalene (47 mg, 0.33 mmol) for 1 h. Reaction was purified by silica with the solvents 98:2 EtOAc:NEt_3, then 90:10 EtOAc:NEt_3. Product was crystalized from warm EtOAc as brown crystals in 52% yield. mp = 165−6 °C, ^{1}H NMR (300 MHz, $CDCl_3$) δ 8.0−8.2 (m, 4H), 7.91 (dd, 1, 8 Hz, 1H), 7.87 (s, 1H), 7.74 (d, 8 Hz, 1H), 7.4−7.6 (m, 4H), 7.4 (m, 2H), 4.61 (dd, 4, 13 Hz, 1H), 4.00 (dd, 9, 14 Hz, 1H), 2.89 (d, 11 Hz, 1H), 2.50 (s, 3H), 2.44 (m, 1H), 2.18 (m, 1H), 1.0−1.8 (m, 11H). Anal. ($C_{26}H_{27}N_3O$·0.1EtOAc) C, H, N.

3-(Carboxy-*N*-decahydroquinoline)-1-(*N*-methylpiperidin-2-ylmethyl)indole (9l). 3-(Carboxylic acid)-1-(*N*-methylpiperidin-2-ylmethyl)indole (112.7 mg, 0.412 mmol) was stirred at room-temperature overnight with 92 μL thionyl chloride and 1 mL methylene chloride, evaporated, and stirred with 1 mL methylene chloride, 62 μL NEt_3, and decahydroquinoline (55.4 mg, 0.399 mmol) for 1 h. Reaction was purified by silica with the solvents 98:2 EtOAc:NEt_3, then 90:10 EtOAc:NEt_3. Product was recovered as a thick oil in 52% yield. ^{1}H NMR (300 MHz, $CDCl_3$) δ 7.71 (dd, 5, 7 Hz, 1H), 7.44 (d, 2 Hz, 1H), 7.35 (d, 8 Hz, 1H), 7.15−7.25 (m, 2H), 4.55 (dd, 4, 14 Hz, 1H), 3.91 (dd, 9, 14 Hz, 1H), 3.4−3.8 (m, 3H), 2.89 (d, 11 Hz, 1H), 2.48 (s, 3H), 2.37 (m, 2H), 2.15 (dt, 4, 11 Hz, 1H), 0.8−1.9 (m, 24H). Anal. ($C_{25}H_{35}N_3O$) C, H, N.

4-(2-Triisopropylsiloxyethyl)naphthoic Acid (15). 4-(2-Triisopropylsiloxyethyl)-1-bromonaphthalene (**14**) was prepared from 4-(2-hydroxyethyl)-1-bromonaphthalene[34] (2.554 g, 10.17 mmol), imidazole (2.788 g, 40.95 mmol), triisopropylsilyl chloride (3.091 g, 20.51 mmol), and 2 mL DMF. The reaction was complete after 2 h slowly heating to 85 °C. After dilution in hexane and washing with DI water, **14** was recovered pure in 99% yield. 2.5 M *n*-butyllithium (1.0 mL, 2.5 mmol) was diluted in 10 mL THF. **14** (1.001 g, 2.458 mmol) and 15 mL anhydrous THF were added to the solution of *n*-butyllithium at −78 °C dropwise over 30 min. The mixture was stirred for 3 h at −78 °C and then dried. CO_2 was allowed to condense over the reaction. Reaction was continued for 15 min with CO_2 flow, warmed to room temperature, and diluted with ether, and then 1 M HCl was added until acidic. The reaction mixture was extracted with ether 2 × 20 mL, brine added, and the mixture extracted again with 20 mL ether, dried with magnesium sulfate, filtered, and evaporated under vacuum. Product (**15**) (451 mg, 1.21 mmol) was purified with flash chromatography using 70:30 hexane:EtOAc. ^{1}H NMR (300 MHz, $CDCl_3$) δ 10.7(vb, 1H), 9.13 (dd, 1.3, 9.0 Hz, 1H), 8.31 (d, 7.5 Hz, 1H), 8.13 (d, 8.1 Hz, 1H) 7.54−7.68 (m, 2H), 7.46 (d, 7.5 Hz, 1H), 7.27−7.38 (m, 5H), 4.55(s, 2H), 3.87(t, 7.2 Hz, 2H), 3.48 (t, 7.2 Hz, 2H).

3-(4-(2-Triisopropylsiloxyethyl)naphthoyl)-1-(*N*-methylpiperidin-2-ylmethyl)indole (21). 21 was obtained by the same method as **19** using **15** (248.9 mg, 0.6681 mmol) and 0.14 mL oxalyl chloride. Then **10** (173.1 mg, 0.7578 mmol) and ([bmin][PF_6])[23] (228 mg) were heated to 100 °C for 14 h. **21** (124.4 mg, 0.2134 mmol) was isolated pure by flash chromatography using 8:2:1 hexane:$CHCl_3$:NEt_3. ^{1}H NMR (300 MHz, $CDCl_3$) δ 8.48 (dd, 3, 6 Hz, 1H), 8.25 (d, 8 Hz, 1H), 8.11 (d, 8 Hz, 1H) 7.2−7.6 (m, 13H), 4.58 (s, 2H), 4.52 (m, 1H) 3.89 (t, 7 Hz, 2H), 3.82 (dd, 9, 14 Hz, 1H), 3.48 (t, 7 Hz, 2H), 2.83 (d, 12H, 1H), 2.39 (s, 3H), 2.45 (b, 1H), 2.09 (dt, 3, 11 Hz, 1H), 0.8−1.7 (m, 9H).

3-(4-(2-Hydroxyethyl)naphthoyl)-1-(*N*-methylpiperidin-2-ylmethyl)indole (9g). 21 (124.4 mg, 0.2134 mmol) was stirred in anhydrous THF with tetrabutylammonium fluoride (68 mg, 0.26 mmol) at 100 °C for 2 h. The pure product (60.4 mg, 0.103 mmol) was obtained by flash chromatography with 3:7:1 hexane:$CHCl_3$:NEt_3 solvent system. ^{1}H NMR (300 MHz, $CDCl_3$) δ 8.31 (dd, 3, 6 Hz, 1H), 8.08 (d, 8 Hz, 1H), 7.97 (d, 8 Hz, 1H) 7.2−7.5 (m, 8H), 4.37 (d, 8 Hz, 1H), 3.90 (t, 2H) 3.68 (m, 1H), 3.36 (d, 14 Hz, 1H), 3.27 (t, 7 Hz, 2H), 2.68 (d, 12H, 1H), 2.24 (s, 3H), 2.45 (b, 1H), 2.09 (t, 11 Hz, 1H), 0.6−1.6 (m, 9H). Anal. ($C_{28}H_{30}N_2O_2$·0.4EtOAc) C, H, N.

3-(6-Benzyloxynaphthoyl)-1-(*N*-methylpiperidin-2-ylmethyl)indole (20). 6-Hydroxynaphthoic acid was alkylated with benzyl bromide and KOH in DMF at 100 °C for 2 h, giving an unoptimized yield of 13% of 6-benzyloxynaphthoic acid benzyl ester. 6-Benzyloxynaphthoic acid benzyl ester (246 mg, 0.714 mmol) was refluxed for 32 h in 5 mL THF and 1 g NaOH in 5 mL water. The product was diluted with 25 mL water, washed with 25 mL ether two times, acidified with HCl, and extracted into ether. 6-Benzyloxynaphthoic acid (**18**) (135.7 mg, 0.488 mmol) was dried and determined to be pure. **20** was obtained by the same method as for **19**, using **18** (124.1 mg, 0.4459 mmol), 0.5 mL thionyl chloride, and then ([bmin][PF_6]) (300 mg) and **10** (103.1 mg, 0.4514 mmol). The mixture was heated to 155 °C for 30 min in a sealed vessel. **20** (42.2 mg, 0.1098 mmol) was purified by flash chromatography 8:2:1 hexane:$CHCl_3$:NEt_3. R_f 0.09. ^{1}H NMR (300 MHz, $CDCl_3$) δ 8.44 (m, 2H), 8.33 (m, 1H), 7.65 (d, 8 Hz, 1H) 7.3−7.6 (m, 11H), 5.33 (s, 2H), 4.53 (dd, 4, 14 Hz, 1H), 3.85 (dd, 9, 14 Hz, 1H), 2.85 (d, 12H, 1H), 2.41 (s, 3H), 2.36 (b, 1H), 2.12 (dt, 3, 12 Hz, 1H), 0.8−1.7 (m, 9H).

3-(6-Hydroxynaphthoyl)-1-(*N*-methylpiperidin-2-ylmethyl)indole (9h). **9h** was obtained by the same method as for **9e**, using **20** (31.0 mg, 0.0806 mmol), 64 mg 10% Pd/C, and 42 mg ammonium formate for 0.5 h. The product was recovered as an oily solid in 90% yield. TLC conditions 5:5:1 hexane:$CHCl_3$:NEt_3 R_f 0.08. ^{1}H NMR (300 MHz, $CDCl_3$) δ 8.46 (dd, 3, 6 Hz, 1H), 8.14 (d, 9 Hz, 1H), 7.84 (d, 8 Hz, 1H) 7.2−7.6 (m, 13H), 4.52 (dd, 4,14 Hz, 1H), 3.86 (dd, 9, 14 Hz, 1H), 2.57 (d, 12H, 1H), 2.40 (s, 3H), 2.35 (b, 1H), 2.09 (dt, 3,12 Hz,

1H), 0.8−1.6 (m, 9H). Anal. ($C_{26}H_{26}N_2O_2 \cdot 1.5H_2O \cdot 1.4HCOOH$) C, H, N.

Radiochemistry. 3-(4-[^{18}F]flouronaphthoyl)-1-(*N*-methylpiperidin-2-ylmethyl)indole ([^{18}F]**9b-1**, [^{18}F]**9b-2**). An aqueous solution of [^{18}F]fluoride, Kryptofix 222 (23 mg), and K_2CO_3 (4.3 mg) was added to a 10 mL vessel. Water was removed by repeated azeotropic evaporations with MeCN at 120 °C and a stream of argon. 4.0 mg of the nitro precursor **9n** and 0.8 mL DMSO were added to the vessel and heated to 160 °C for 18 min. The reaction was cooled, dissolved in 1 mL of the mobile phase, injected onto a 7.8 × 300 mm Symmetry reverse phase HPLC column, and eluted with 300:700:2 THF:H_2O:TFA at a flow rate of 4.5 mL/min. The radioactive peak was collected, evaporated, diluted with 100 μL mobile phase, and then injected on a 4.6 × 250 mm Chiralcel OD column with a 75:25:0.2 hexane:IPA:diethylamine mobile phase at 1.1 mL/min. This procedure separated the enantiomers with nearly 3 min of baseline resolution between the two enantiomers. The two enantiomers [^{18}F]**9b-1** and [^{18}F]**9b-2** came out at 7.4 and 11.7 min with the second peak being the active isomer.

Molecular Modeling. The dipole moment was determined using the Chemdraw3D software package. The minimum energy conformation of compound **8** was found by several conformational energy searches. An initial conformational energy search was performed, then Torsion 1 (indole C2, C3, carbonyl carbon, and naphthyl C1) (numbering found in Figure 5) was rotated 180° and a conformational energy search was repeated. The same was done with Torsion 2 (indole C3, carbonyl carbon, naphthyl C1, and C2). The minimum energy conformation for Torsion 1 and Torsion 2 was used to find the minimum energy conformation for Torsion 3 (indole C2, N1, tail CH_2, and CH). Torsion 3 was rotated 60°, a conformational energy search was performed and the process was repeated three times. The lowest energy conformation of **8** was modified to determine the rest of the ligands in this set.

Distribution of Radioactivity in the Mouse Brain. All experiments with research animals were approved by the Animal Care and Use Committee of the NIDA Intramural Research Program. Male CD-1 mice weighing 25−35 g (Charles River Laboratories, Wilmington, MA) received an injection of a known amount of the radiotracer (5−7 μCi in 200 μL saline, specific activity 2400−3200 Ci/mmol) into the lateral tail vein**.** The mass of injected radioligands ranged from 0.06 to 0.07 nmol/kg. In the blocking studies, animals were administered with nonradioactive **5** (1 mg/kg, sc) 15 min before radioligand injection. Animals were euthanized by cervical dislocation at predetermined intervals (n = 3 for each time point) after injection of the radioligand. The brains were removed quickly from the skull and dissected. Samples were weighed and their radioactivity assayed in a γ counter (Cobra, Packard Instruments, Meriden, CT). The accumulation of radioactivity in the brain samples was calculated as the amount of radioactivity per gram of tissue and expressed as the percentage of the administered radiotracer dose per kg of body weight.

Radioligand in Vitro Binding Assays. Competition binding assays were carried out with [^{3}H]**2** (168 Ci/mmol, Perkin-Elmer, MA) and rat cerebellum membrane fraction. The membrane fraction was prepared from frozen Sprague−Dawley rat cerebellum tissue (Pel-Freez Biologicals) as described previously.[14] On the day of assay, the pellet was resuspended in ice-cold assay buffer (pH = 7.4), containing 50 mM TrisHCl, 3 mM $MgCl_2$, 1 mM EDTA, and 0.5% fat free bovine serum albumin.

Aliquots of membrane fraction corresponding to 0.6 mg of cerebellum tissue were incubated at 30 °C for 1 h with 0.5 nM [^{3}H]**2** and serial dilutions of test drugs in a total incubation volume of 0.8 mL. All assays were performed in glass test tubes. Nonspecific binding was determined in the presence of 0.5 mM of **2** (Tocris Cookson Inc., UK). Binding was terminated by vacuum filtration through GF/C filters pretreated in the rinse buffer. The rinse buffer used was 50 mM Tris-HCl containing 0.5% of nonfat dry milk to reduce nonspecific binding to filter material. Radioactivity was measured using a liquid scintillation counter (Beckman LS 6000, 37% efficiency). All assays were carried out in quadruplicate. The K_i values were calculated by the Cheng−Prusoff equation based on the measured IC_{50} values and K_d = 0.5 nM for the binding of [^{3}H]**2**. The K_d value for [^{3}H]**2** was determined in the same conditions using serial dilutions of [^{3}H]**2** with nonradiactive **2**.

Acknowledgment. The authors thank Drs. Elliot Stein, Amy H. Newman, Alex Hoffman, and Reeti Katoch-Rouse for their helpful discussions, and Ms. Mary Pfeiffer for her kind editorial assistance.

Supporting Information Available: Elemental analysis results and ^{1}H NMR spectra for pure final compounds is available free of charge via the Internet at http://pubs.acs.org.

References

(1) Howlett, A. C.; Barth, F.; Bonner, T. I.; Cabral, G.; Casellas, P.; Devane, W. A.; Felder, C. C.; Herkenham, M.; Mackie, K.; Martin, B. R.; Mechoulam, R.; Pertwee, R. G. International Union of Pharmacology. XXVII. Classification of cannabinoid receptors. *Pharmacol. Rev.* **2002**, *54*, 161−202.
(2) Cabral, G. A. *Marijuana and the immune system*; Humana Press: Totowa, NJ, 1999.
(3) Martin, B. R.; Mechoulam, R.; Razdan, R. K. Discovery and characterization of endogenous cannabinoids. *Life Sci.* **1999**, *65*, 573−595.
(4) Makriyannis, A.; Goutopoulos, A. Cannabinergics: old and new theraputic possibilities. In *Drug discovery strategies and methods*; Makriyannis, A., Biegel, D., Eds.; Marcel Dekker: New York, 2004; pp 89−128.
(5) Le Foll, B.; Goldberg, S. R. Cannabinoid CB1 Receptor Antagonists as Promising New Medications for Drug Dependence. *J. Pharmacol. Exp. Ther.* **2005**, *312*, 875−883.
(6) Levitt, M. Cannabinoids as antiemetics in cancer chemotherapy. In *Cannabinoids as therapeutic agents*; Mechoulam, R., Ed.; CRC Press: Boca Raton, FL, 1986; pp 73−79.
(7) Arnone, M.; Maruani, J.; Chaperon, F. Selective inhibition of sucrose and ethanol intake by SR141716a, an antagonist of central cannabinoid receptors. *Psychopharmacology* **1998**, *132*, 104−106.
(8) Sieradzan, K. A.; Fox, S. H.; Hill, M.; Dick, J. P.; Crossman, A. R.; Brotchie, J. M. Cannabinoids reduce levodopa-induced dyskinesia in Parkinson's disease: A pilot study. *Neurology* **2001**, *57*, 2108−2111.
(9) Mathews, W. B.; Scheffel, U.; Finley, P.; Ravert, H. T.; Frank, R. A.; Rinaldi-Carmona, M.; Barth, F.; Dannals, R. F. Biodistribution of [^{18}F] SR144385 and [^{18}F] SR 147963: Selective radioligands for positron emission tomographic studies of brain cannabinoid receptors. *Nucl. Med. Biol.* **2000**, *27*, 757−762.
(10) Mathews, W. B.; Scheffel, U.; Rauseo, P. A.; Ravert, H. T.; Frank, R. A.; Ellames, G. J.; Herbert, J. M.; Barth, F.; Rinaldi-Carmona, M.; and Dannals, R. F. Carbon-11 labeled radioligands for imaging brain cannabinoid receptors. *Nucl. Med. Biol.* **2002**, *29*, 671−677.
(11) Gatley, S. J.; Lan, R.; Volkow, N. D.; Pappas, N.; King, P.; Wong, C. T.; Gifford, A. N.; Pyatt, B.; Dewey, S. L.; Makriyannis, A. Imaging the brain marijuana receptor: development of a radioligand that binds to cannabinoid CB1 receptors in vivo. *J. Neurochem.* **1998**, *70*, 417−423.
(12) Gatley, S. J.; Gifford, A. N.; Volkow, N. D.; Lan, R.; Makriyannis, A. ^{123}I-labeled AM251: a radioiodinated ligand which binds in vivo to mouse brain cannabinoid CB1 receptors. *Eur. J. Pharmacol.* **1996**, *307*, 331−338.
(13) Cosenza, M.; Gifford, A. N.; Gatley, S. J.; Pyratt, B.; Liu, Q.; Makriyannis, A.; Volkow, N. D. Locomotor activity and occupancy of brain cannabinoid CB1 receptors by the antagonist/inverse agonist AM281. *Synapse* **2000**, *38*, 477−482.
(14) Katoch-Rouse, R.; Pavlova, O. A.; Caulder, T.; Hoffman, A. F.; Mukhin, A. G.; Horti, A. G. Synthesis structure−activity relationship, and evaluation of SR141716 analogues: Development of central cannabinoid receptor ligands with lower lipophilicity. *J. Med. Chem.* **2003**, *46*, 642−645.
(15) Lan, R.; Gatley, S. J.; Makriyannis, A. Preparation of iodine-123 labeled AM251: a potential SPECT radioligand for the brain cannabinoid CB1 receptors. *J. Labelled Compd. Radiopharm.* **1996**, *38*, 875−881.
(16) D'Ambra, T. E.; Eissenstat, M. A.; Abt, J.; Ackerman, J. H.; Bacon, E. R.; Bell, M. R.; Carabateas, P. M.; Josef, K. A.; Kumar, V.; Weaver, J. D.; Arnold, R.; Casiano, F. M.; Chippari, S. M.; Haycock, D. A.; Kuster, J. E.; Luttinger, A.; Stevenson, J. I.; Ward, S. J.; Hill, W. A.; Khanolkar, A.; Makriyannis, A. C-Attached aminoalkylindoles: potent cannabinoid mimetics. *Bioorg. Med. Chem. Lett.* **1996**, *6*, 17−22.

(17) Tetko, I. V.; Kovalishyn, V. V.; Livingstone, D. J. Volume learning algorithm artificial neural networks for 3D QSAR studies. *J. Med. Chem.* **2001**, *44*, 2411−2420.
(18) Deng, H. Design and synthesis of selective cannabinoid receptor ligands: Aminoalkylindole and other heterocyclic analogs. Ph.D. Dissertation, University of Connecticut, Storrs, CT, 2000.
(19) Makriyannis, A.; Deng, H. Cannabimimetic indole derivatives. WO 2001/028557.
(20) Wilson, A. A.; Jin, L.; Garcia, A.; DaSilva, J. N.; Houle, S. An admonition when measuring the lipophilicity of radiotracers using counting techniques. *Appl. Radiat. Isot.* **2001**, *54*, 203−208.
(21) Shim, J.; Collantes, E. R.; Welsh, W. J. Three-dimensional quantitative structure−activity relationship study of the cannabimimetic (aminoalkyl)indoles using comparative molecular field analysis. *J. Med. Chem.* **1998**, *41*, 4521−4532.
(22) Kandemirli, F. Structure−activity relationships investigation in a mixed series of cannabiniods. *Arzneim.-Forsch./Drug Res.* **2002**, *52*, 731−739.
(23) Earle, M. J.; McCormac, P. B.; Seddon, K. R. The first high yield route to a pharmaceutical in a room-temperature ionic liquid. *Green Chem.* **2000**, *2*, 261−262.
(24) Makriyannis, A.; Liu, Q. Heteroindanes: a new class of potent cannabimimetic ligands. WO 2003/035005.
(25) Leftheris, K.; Zhao, R.; Chen, B.; Kiener, P.; Wu, H.; Pandit, C.; Wrobleski, S.; Chen, P.; Hynes, J.; Longphre, M.; Norris, D. J.; Spergel, S.; Tokarski, J. Cannabinoid receptor modulators, their processes of preparation, and use of cannabinoid receptor modulators for treating respiratory and non-respiratory diseases. WO 2001/058869.
(26) Carreño, M. C.; Ruano, J. L.; Sanz, G.; Toledo, M. A.; Urbano, A. *N*-bromosuccinimide as a regioselective nuclear monobrominating reagent for phenols and naphthols. *Synlett* **1997**, 1241−1242.
(27) Berridge, M. S.; Crouzel, C.; Comar, D. Aromatic fluorination with n.c.a. 18F-fluoride: a comparative study. *J. Labelled Compd. Radiopharm.* **1985**, *22*, 687−691.
(28) Herkenham, M.; Lynn, A. B.; Little, M. D.; Johnson, M. R.; Melvin, L. S.; DeCosta, B. R.; Rice, K. C. Cannabinoid receptor localization in brain. *Proc. Natl. Acad. Sci. U.S.A.* **1990**, *87*, 1932−1936.
(29) Herkenham, M.; Lynn, A. B.; Little, M. D.; Johnson, M. R.; Melvin, L. S.; DeCosta, B. R.; Rice, K. C. Characterization and localization of cannabinoid receptors in rat brain: a quantitative in vitro autoradiographic study. *J. Neurosci.* **1991**, *11*, 563−583.
(30) Blicke, F. F.; Gomberg, M. Triphenyhnethyl. XXXIII. Quinoidation in the triarylmethyls. *J. Am. Chem. Soc.* **1923**, *45*, 1765.
(31) Dewar, M. J.; Grisdale, P. J. Substituent Effects. The Preperation of a series of substituted 1-Naphthoic acids. *J. Chem. Soc.* **1962**, 3541−3546.
(32) Resch, J. F.; Lehr, G. S.; Wischik, C. M. Design and synthesis of a potential affinity/cleaving reagent for beta-pleated sheet protein structures. *Bioorg. Med. Chem. Lett.* **1991**, *1*, 519−522.
(33) Ried, W.; Schön, M. Abfangreaktionen von Dehydrobenzol mit Diazoketonen. *Liebigs Ann. Chem.* **1965**, 141−144.
(34) Olah, G. A.; Singh, B. P.; Liang, G. Stable carbocations. 255. α-Ethylenehaloarenium ions. *J. Org. Chem.* **1984**, *49*, 2922−2925.

JM0502743